https://doi.org/10.5194/tc-2020-36
Preprint. Discussion started: 11 February 2020

The Cryosphere Discussions

Reconciling the surface temperature–surface mass balance relationship in models and ice cores in Antarctica over the last two centuries

Marie G.P. Cavitte[1], Quentin Dalaiden[1], Hugues Goosse[1], Jan T.M. Lenaerts[2], and Elizabeth R. Thomas[3]

[1]Georges Lemaître Centre for Earth and Climate Research (TECLIM), Earth and Life Institute (ELI), Université catholique de Louvain (UCL), Louvain-la-Neuve Belgium
[2]Department of Atmospheric and Oceanic Sciences, University of Colorado Boulder, Boulder CO, USA
[3]British Antarctic Survey, Madingley Road, Cambridge, CB3 0ET, UK

Correspondence: Marie G.P. Cavitte (marie.cavitte@uclouvain.be)

Abstract. Ice cores are an important record of the past surface mass balance (SMB) of ice sheets, with SMB mitigating the ice sheets' sea level impact over the recent decades. For the Antarctic Ice Sheet (AIS), SMB is dominated by large-scale atmospheric circulation, which collects warm moist air from further north and releases it in the form of snow as widespread accumulation or focused atmospheric rivers on the continent. This implies that the snow deposited at the surface of the AIS should record strongly coupled SMB and surface air temperature (SAT) variations. Ice cores use δ^{18}O as a proxy for SAT as they do not record SAT directly. Here, using isotope-enabled global climate models and the RACMO2.3 regional climate model, we calculate positive SMB-SAT and δ^{18}O-SMB correlations over ~90% of the AIS. The high spatial resolution of the RACMO2.3 model allows us to highlight a number of areas where SMB and SAT are not correlated, and show that wind-driven processes acting locally, such as Foehn and katabatic effects, can overwhelm the large-scale atmospheric input in SMB and SAT responsible for the positive SMB-SAT correlations. We focus in particular on Dronning Maud Land, East Antarctica, where the ice promontories clearly show these wind-induced effects. However, using the PAGES2k ice core compilations of SMB and δ^{18}O of Thomas et al. (2017) and Stenni et al. (2017), we obtain a weak correlation, on the order of 0.1, between SMB and δ^{18}O over the past ~150 years. We obtain an equivalently weak correlation between ice core SMB and the SAT reconstruction of Nicolas and Bromwich (2014) over the past ~50 years, although the ice core sites are not spatially co-located with the areas displaying a low SMB-SAT correlation in the models. To resolve the discrepancy between the measured and modeled signals, we show that averaging the ice core records in close spatial proximity increases their SMB-SAT correlation. This increase shows that the weak measured correlation likely results from random noise present in the ice core records, but is not large enough to match the correlation calculated in the models. Our results indicate thus a positive correlation between SAT and SMB in models and ice core reconstructions but with a weaker value in observations that may be due to missing processes in models or some systematic biases in ice core data that are not removed by a simple average.

https://doi.org/10.5194/tc-2020-36
Preprint. Discussion started: 11 February 2020

The Cryosphere Discussions

1 Introduction

In the context of current climate change and sea level rise (SLR) in the last century, it is important to better constrain the future contributions from the Antarctic Ice Sheet (AIS) to SLR, projected to be the largest source of sea-level rise over centennial to millenial timescales, with 58.3 m of potential SLR if the entire ice sheet were to melt (Stocker et al., 2013; Pörtner et al., in press). To better predict the timing and rate of the AIS contributions to SLR, we need to better constrain its mass balance. The grounded AIS mass balance is the difference between surface mass balance (SMB), i.e. the addition of mass at the surface of the ice sheet, and ice discharge through basal hydrology and calving (Lenaerts et al., 2019). The AIS mass balance is currently negative due to increased ice discharge at the grounding lines (Shepherd et al., 2018), particularly enhanced in the Amundsen Sea Embayment (Mouginot et al., 2014; Rignot et al., 2019), outpacing SMB. SMB could play a bigger role in mitigating future SLR, but it is still not well understood. For the AIS, the SMB signal is generally dominated by snow accumulation (Agosta et al., 2019; Van Wessem et al., 2018). The main SMB sinks for the AIS are sublimation and wind ablation and melt water runoff, although the latter is negligible for the AIS due to the very low surface temperatures.

Large-scale atmospheric circulation strongly controls SMB in Antarctica, bringing air masses with a high moisture and temperature content (Lenaerts et al., 2019). This large-scale (100s of km) atmospheric circulation usually embeds synoptic-scale cyclones that collect heat and moisture from further north, including the Southern Ocean, which they can release onto the AIS (Gorodetskaya et al., 2014; Sodemann and Stohl, 2009; Wang et al., 2019). SMB shows a large coast-to-interior gradient with very low SMB values in the continental interior (Scarchilli et al., 2011; Fujita et al., 2011; Favier et al., 2013; Frezzotti et al., 2007), although atmospheric rivers can bring mid-latitude moisture very deep into the interior (Gorodetskaya et al., 2014). Large-scale atmospheric modes of variability dominate snow accumulation in Antarctica (Lenaerts et al., 2019). Notably, the Southern Annular Mode has been shown to have a dominant role in driving snow accumulation, particularly in the Antarctic Peninsula (Thomas et al., 2008, 2015, 2017) and to largely explain the observed SMB patterns across the entire AIS during the 20th century (Medley and Thomas, 2019). In addition, based on the Clausius-Clapeyron relationship, the increasing surface air temperature (SAT) due to climate change should induce a greater moisture holding capacity of the air, and therefore increased snowfall (Frieler et al., 2015) with increased SAT. If this predicted increase in SMB is linked to increasing SAT in the 21st century, it will be interesting to see if SMB and SAT are linked in the past too, in which case SMB records over time will be a helpful tool to constrain past climates.

Ice cores provide an important local and regional record of snow accumulation (Thomas et al., 2017), while the δ^{18}O measured in the ice cores is often used as a proxy for SAT (Stenni et al., 2000; Frieler et al., 2015). The SMB and SAT records should be correlated, regardless of whether SMB is controlled by the Clausius-Clapeyron law or by synoptic-scale atmospheric circulation. Several studies have already shown SMB and δ^{18}O to co-vary in ice cores and SMB and SAT to co-vary in models in specific AIS regions. Medley et al. (2018) calculate a sensitivity between SMB and SAT around 19 mm w.e. $^{\circ}C^{-1}$ over Queen Maud Land using global atmospheric models, Frezzotti et al. (2004) measure a linear snow accumulation increase of ~15 mm w.e. per °C increase in firn temperature in ice cores over Adélie Land and Frieler et al. (2015) observe and model a linear increase ranging from ~4.5 to 7% K^{-1} over the AIS. However, Medley and Thomas (2019) have recently shown that,

https://doi.org/10.5194/tc-2020-36
Preprint. Discussion started: 11 February 2020


The Cryosphere Discussions
Open Access
EGU

despite a continent-wide temperature warming, SMB trends vary strongly spatially at the continent scale. Both the ice core records and the models used in the study point to a complex SMB-SAT relationship. Dalaiden et al. (2019) have described the co-variance of SMB-SAT on millennial and centennial timescales for seven distinct Antarctic regions. However, the same authors already display a large discrepancy in the strength of the co-variance at this continental scale between the ice core records and the model predictions.

Added complexity in snow accumulation records originates from smaller-scale (several kilometers or less) wind-based redistribution of snow that is superimposed on large-scale atmospheric circulation accumulation sources. We will refer to this wind-based redistribution as the "local-scale". Wind speeds that reach a threshold speed (~5 m s^{-1}) can pluck snow from the surface and redeposit it up to several kilometers away where winds decelerate or remove it through blowing snow sublimation (Frezzotti et al., 2004; King et al., 2004; Lenaerts et al., 2019; Agosta et al., 2019). Due to the temperature inversion that commonly occurs near the surface of the ice sheet, the surface air is negatively buoyant and flows down-slope through the influence of gravity (van den Broeke et al., 2002). Whillans (1975) shows a strong relationship between slope, wind strength and mass drift transport. With increased distance and steepness of slope, these dry cold air masses originating from the interior accelerate significantly as they flow down towards the coast, the so-called katabatic winds (Bromwich, 1989; Bromwich and Liu, 1996), reaching speeds of 19.4 m s^{-1} in Adélie Land (van den Broeke et al., 2002), and up to 90 m s^{-1} measured at Cape Denison (Ball, 1957). Katabatics can cause widespread snow redistribution over kilometers and thus affect the local SMB.

Winds can also impact surface accumulation over shorter spatial scales (10s of meters to kilometers) when they flow over surface topography. As surface winds flow over surface topography, they typically erode the windward side and deposit on the leeward side, thus reworking the SMB record spatially (Black and Budd, 1964; Budd, 1971; Dattler et al., 2019). If winds are very persistent in direction and speed, wind redistribution of the snow pack can create fields of dunes (Frezzotti et al., 2002b; Arcone et al., 2012a; Das et al., 2013) or blue ice areas (Spaulding et al., 2012). Winds also have a strong effect on SAT at the local-scale and therefore affect the co-variance of SMB-SAT. Lenaerts et al. (2017) show that persistent katabatic winds on the Dronning Maud Land (DML) coast can warm the air temperature through enhanced air column mixing at the grounding line.

An additional influence on SAT at the local-scale, but also at large-scale, is when large-scale (synoptic) winds interact with surface topography that acts as an obstacle to air flow. A thermodynamic effect will occur, known at the Foehn effect. This Foehn effect can occur across mountain ranges (e.g. the Trans-Antarctic Mountains) or isolated bumps (e.g. ice promontories or ice rises). Cooling and condensation during uplift of the air mass will remove moisture which implies latent heating of the air and results in warmer air descending on the lee side of the surface topography (Elvidge et al., 2015; Elvidge and Renfrew, 2016). This has been well documented for the AP (Datta et al., 2018, 2019).

Our work follows from that of (Dalaiden et al., 2019), in which they show that SMB and SAT are strongly correlated at the continental scale over historical timescales. Here, we examine whether the relationship remains strong at the model grid point scale (which we refer to as the regional scale) and the ice core scale (referred to hereafter as the local scale). For this, we use a suite of Global Climate Models (GCM), a Regional Climate Model (RCM) and published ice core compilations available for the AIS. Combining both in-situ measurements and model simulations allows us to characterise the SMB-SAT relationship over these different spatial scales. In summary, we want to understand the following aspects of the link between SAT and SMB:

https://doi.org/10.5194/tc-2020-36
Preprint. Discussion started: 11 February 2020

1. Which processes link SAT and SMB at regional scales and how do they scale down from conclusions at the continental scale

2. How does the SMB-SAT link in models at the regional scale compare to that in ice cores at the local scale

3. Can our improved understanding of processes at the regional scales explain why the SMB-SAT link measured in ice cores is different to the link as measured in models

We start with a brief description of the data sets and models used in this study. Then we compare the SMB-SAT relationship, as well the SMB-δ^{18}O relationship, obtained in the models at regional scale to compare to continental-scale results of Dalaiden et al. (2019). We hypothesize physical mechanisms that could explain the discrete areas of the AIS where the SMB-SAT relationship is weak. We then examine the SMB-SAT relationship in the ice core data, and attempt to reconcile the differences between the results at this local scale and those from the models at the regional scale.

2 Methods and Data

2.1 Isotopic global climate models

To study longer-term regional climate variability, we use modeled SMB and SAT from four isotope-enabled GCMs (iGCMs hereafter) taken from the Coupled Model Intercomparison Project Phase 5 (CMIP5). These were chosen specifically because (1) they have historical simulations for the required variables (SAT, and precipitation and sublimation/evaporation for SMB), (2) they simulate water isotope variations (δ^{18}O) explicitly, which can be compared directly to water isotopes from the ice cores and (3) for consistency with those used in the Dalaiden et al. (2019) study (with the additional fourth made available recently, Brady et al. (2019)). The iGCM characteristics are detailed in Dalaiden et al. (2019) but we describe their relevant characteristics to this study briefly:

- ECHAM5-MPI/OM is a fully coupled GCM that includes atmospheric and oceanic components, and covers the period 800–2000 AD. It is forced by natural and anthropogenic forcing (Sjolte et al., 2018) and has a spatial resolution of 3.75° × 3.75° (for the atmospheric component).

- ECHAM5-wiso is a GCM that only includes an atmospheric component and covers the period 1871–2011 AD driven by a sea surface temperatures and sea ice (Rayner et al., 2003) at a spatial resolution of ~1° (Steiger et al., 2017).

- iHadCM3 is the isotope-enabled version of the fully coupled version of GCM HadCM3 (Turner et al., 2016; Holloway et al., 2016) and covers the period 1851–2003 AD at a spatial resolution of 3.75° × 2.5° (for the atmospheric component).

- iCESM1 is an isotope-enabled version of CESM1 (Brady et al., 2019). It has active atmosphere, land, ocean, river transport and sea ice model components, with a spatial resolution of ~2° for the atmospheric model. The simulations cover 850–2005 AD. iCESM1 is an addition to the iGCM model list of the Dalaiden et al. (2019) study.

https://doi.org/10.5194/tc-2020-36
Preprint. Discussion started: 11 February 2020

Because iCESM1 and iHadCM3 have three and seven simulations, respectively (each has slightly different initial conditions), we average over their ensemble of simulations to obtain a mean representation of SMB, SAT and δ^{18}O for each iGCM. Although there are slight spatial differences, all four iGCMs show similar spatial variations of the correlation between SMB-SAT and δ^{18}O-SMB on the continent scale (see Fig.S1-S4, Dalaiden et al. (2019) provide an evaluation of the iGCMs used here). To compare the iGCM continent-wide correlations to the RCM-derived correlations, we interpolate the iGCM results onto the RCM grid and average over all four iGCMs. P-values are not interpolated but rather a threshold of at least 50% of p-values < 0.1 is used to define whether a grid point correlation value is significative. Note that we choose a threshold p-value of 0.1 due to the short length of some data sets. The individual iGCM correlation results can be found in supplementary Fig.S1-S4.

In this study, we focus on two time intervals for the iGCMs: a longer (~150 year) timescale covering 1871–2000 AD to compare to the measured ice core SMB and δ^{18}O data, and a shorter (~40 years) timescale covering 1961–2000 AD for comparison to the RCM simulations and measured SAT. To ensure that a shorter time interval does not impact the correlations, we calculate the δ^{18}O-SMB and SMB-SAT correlations over the 1871–2000 AD and the 1961–2000 AD intervals for the iGCMs. We show that both correlations are very similar over the two time intervals, both in spatial distribution and in continent-wide average (see Fig.1). The main difference is that, due to the shorter time interval, the surface area with a correlation p-value > 0.1 increases.

2.2 RACMO2.3p2 regional climate model

For regional climate variability at a higher spatial resolution, we use the RCM Regional Atmospheric Climate MOdel version 2.3p2 (RACMO2.3 hereafter) which provides SMB, SAT and other relevant atmospheric variables for the entire AIS. RACMO2.3 combines the atmospheric dynamics of the High Resolution Limited Area Model (HIRLAM5, Unden et al., 2002) and the physics package of the European Centre for Medium-range Weather Forecasts (ECMWF, 2009). It is forced at its boundaries by the ERA-Interim reanalysis from ECMWF over 1979–2016 AD. This version of RACMO is coupled to a multi-layer snow model which includes a snow albedo and a drifting snow scheme (Lenaerts et al., 2010), thus making it particularly well suited to studying polar regions. RACMO2.3 has been demonstrated to have the best fit to recent AIS SMB observations compared to other atmospheric and reanalysis models (Wang et al., 2016). A more detailed description of RACMO2.3 can be found in Van Wessem et al. (2018). In this study, we use the 27 km horizontal gridding simulations over the entire AIS (Van Wessem et al., 2018), as well as the 5.5 km horizontal gridding simulations focused on the DML region (~25°W–45°E, Lenaerts et al., 2017). The latter configuration at higher resolution allows studying in more details a region with complex surface topography and SMB records (Lenaerts et al., 2017, 2014, ,etc.). Both RACMO2.3 simulations cover 1979–2016 AD. We will refer to these as RACMO27 and RACMO5 hereafter.

2.3 In-situ measurements

The correlations obtained from the model simulations are compared to in-situ measurements of SMB, SAT and δ^{18}O from ice cores and weather stations.

https://doi.org/10.5194/tc-2020-36
Preprint. Discussion started: 11 February 2020

Ice cores provide a measurement of SMB based on the measured distance between distinct seasonal depth markers within the ice core on historical timescales. The annual layer thickness is corrected for densification, compaction and ice flow to produce a water equivalent snow accumulation. We use the Thomas et al. (2017) compilation, the most comprehensive SMB compilation to date for the AIS. Thomas et al. (2017) use 79 ice cores over the AIS to obtain a SMB record with an annual resolution that covers the last millenium up to 2010 AD.

Ice cores record variations with depth of the ice's δ^{18}O. Here we use the Stenni et al. (2017) compilation (a total of 112 ice cores) over the AIS to obtain a δ^{18}O record that covers the past millennium up to 2014 AD with a 5-year resolution for 0–2014 AD. The ice core δ^{18}O record can also be used as a proxy for SAT. However, studies have shown that δ^{18}O is not a perfect proxy for SAT (Dalaiden et al., 2019; Klein et al., 2019; Goursaud et al., 2017, 2019). Dalaiden et al. (2019) have shown that the correlation between δ^{18}O and SMB was weaker than the correlation of SAT with SMB for seven distinct regions at the continental scale.

Because ice cores do not provide a direct measurement of SAT, we rely on the Nicolas and Bromwich (2014) SAT reconstruction which uses SAT records from 15 weather stations around the AIS (mostly coastal) to calculate an interpolated AIS-wide SAT field. This interpolated SAT field allows us to correlate SAT and SMB directly at the ice core locations so as to compare to the RACMO2.3 results. The Nicolas and Bromwich (2014) reconstruction is limited to the 1958–2012 AD time interval.

In the Thomas et al. (2017) and Stenni et al. (2017) ice core data compilations, most of the ice core records start ~1800 AD, which is why we choose to correlate the SMB and temperature signals over the same timescales as the models, starting in 1871 AD. Furthermore, the spatial distribution of the ice cores over the AIS is not homogeneous, with the majority of the ice cores located in the coastal areas, and very few in the interior (see supplementary Fig.S5). This certainly introduces a spatial bias in our ice core-based correlation towards coastal signals and processes.

3 Results and Discussion

3.1 How do the processes that link SAT and SMB at the continental scale vary at the regional scale?

3.1.1 Strength of the link between SMB and SAT at the regional scale

Dalaiden et al. (2019) have shown that the relationship between SMB and SAT is positive on the continental scale for each of their seven Antarctic regions, whether they used the GCMs or RACMO2.3 simulations. Here, we calculate the annual correlation between SMB and SAT at the regional scale over 1871–2000 AD, the time interval shared by all iGCMs. We obtain a positive annual relationship between SMB and SAT at the regional scale with a continent-wide average value of 0.57 and a spatial standard deviation of $\pm$0.10 (hereafter referred to as $\pm$0.10) over the four iGCMs (the individual iGCMs continent averages range from 0.52-0.59) with a p-value < 0.1 for more than 95% of each GCM's surface area (Fig.1, panel c). Moreover, the maximum and minimum correlations obtained are consistent between iGCMs, in magnitude and spatial distribution (see supplementary Fig.S1-S4). We obtain the same result if we take non-overlapping 5-year averages of the SMB and SAT variables

https://doi.org/10.5194/tc-2020-36
Preprint. Discussion started: 11 February 2020

to calculate their 5-yearly correlation (see supplementary Fig.S6). We repeat the annual correlation of SAT and SMB using the RACMO27 simulations over 1979–2016 AD (see Fig.2). At this spatial scale, the correlation is also positive in the large majority of regions with a similar range of correlation values and a continent-wide average value of 0.54±0.22. Moving down to RACMO5 simulations, the highest spatial model resolution available to us, we show that the correlation in the DML region is also positive, with a regional average value of 0.48±0.18 (comparable to an average value of 0.52±0.21 for RACMO27 for the same region, see Fig.3). This implies that the correlation of SMB and SAT is similar over the 1871–2000 AD and the 1979–2016 AD time intervals, and from a spatial resolution of > 1° down to 5.5 km. Whatever the temporal and spatial scale, the correlation between SMB and SAT is positive for a large majority of the model grid points. It is also true for summer- or winter-only months (average SMB-SAT correlation of 0.43 or 0.56, respectively using RACMO27, see supplementary Fig.S7) or on monthly timescales after removing the seasonal cycle (0.54 on average, see supplementary Fig.S8).

3.1.2 Wind effects on SMB and SAT signals

There are a few areas, spatially consistent between the RACMO27, RACMO5 simulations and the iGCMs, where the SMB-SAT correlation is not as strong. In those areas, shaded in grey on Fig.2 and outlined on subsequent figures, the correlation is either insignificant (p-value > 0.1) or negative. A weak SMB-SAT correlation suggests that physical processes must affect SMB, SAT or both enough locally that they break the relationship between SMB and SAT seen at large scale in other regions. Winds are known to affect SMB and SAT locally, through wind-based redistribution of SMB, turbulent warming from katabatics and Foehn warming effects on leeward slopes. To evaluate whether the lack of correlation between SAT and SMB is due to such wind effects, we correlate modelled surface winds to our two variables of interest.

If we define positive wind direction to be pointing down-slope, we expect wind to be negatively correlated to both SAT and SMB on average. Large-scale air masses, originating over the Southern Ocean and further north, bring warm moist air towards the interior as they flow up-slope, thus inducing a strong and negative correlation. Any area of the AIS that does not show this negative correlation between wind and SAT or SMB implies that the large-scale atmospheric air circulation does not dominate, and evidenced in a weak link between SMB and SAT.

Because wind direction with respect to surface slope and wind strength influence SMB and SAT locally (Frezzotti et al., 2004; King et al., 2004; Black and Budd, 1964; Grima et al., 2014), we take both into account in the Mean (surface) Slope in the (mean) Wind Direction (MSWD). MSWD is defined as the dot product between the mean surface slope and the mean wind direction (Scambos et al., 2012; Das et al., 2013; Dattler et al., 2019):

$$\overrightarrow{MSWD} = \overrightarrow{ws}_{10m} \cdot \overrightarrow{slope} \quad (1)$$

with $\overrightarrow{ws}_{10m}$ the wind speed 10 m above the surface, and define $\overrightarrow{slope}$ as pointing down-slope. Winds flowing down-slope will therefore have a positive MSWD.

Surface slope is calculated using the surface topography used in the RACMO2.3 simulations. As the ratio of vertical distance over horizontal distance, it has units of $m \cdot m^{-1}$, i.e. unitless. We then remove areas of the AIS with a negligible slope (<0.001)

https://doi.org/10.5194/tc-2020-36
Preprint. Discussion started: 11 February 2020

as in these areas, MSWD will be close to null and will introduce a lot of noise when correlating it with SMB or SAT. We then correlate SAT and SMB to this MSWD.

We calculate the correlation of MSWD with both SAT and SMB at the 27 km and 5.5 km scales, using the RACMO27 and RACMO5 simulations, shown on Figs.4 and 5. Examining the results, MSWD is negatively correlated to SAT with a continent-wide average of -0.31 at the 27 km scale, and a DML average of -0.4 at the 5.5 km scale (Fig.4). MSWD is also negatively correlated to SMB with a continent-wide average of -0.6 at the 27 km scale, and a DML average of -0.52 at the 5.5 km scale (Fig.5). Agosta et al. (2019) also show a strong link between modelled surface topography (surface curvature in their case) with SMB over the continent when wind speeds exceed 5 m s^{-1} .

However, a number of areas show a very positive MSWD-SAT correlation simultaneously with a weaker-to-positive MSWD-SMB correlation, that are co-located with the areas where the SMB-SAT correlation is weak (outlined here with a magenta line). Those areas are at roughly the same locations in the 5.5 km and 27 km simulations.

Let us first focus on the link between wind redistribution and SAT. The areas where the SMB-SAT correlation is weak have a strong and positive MSWD-SAT correlation. We note that these areas tend to be on the leeward side of surface topography. The clearest example of this is found along the AP (see Fig.4). Here, Westerlies are the dominant year-around air mass trajectory (Marshall et al., 2006) and the whole eastern side of the AP shows a very positive MSWD-SAT signature aligned along the Trans-Antarctic Mountains. The Trans-Antarctic Mountains create a long barrier perpendicular to the air masses' dominant trajectory. The warmer air masses coming from the ocean are forced up the windward side (MSWD < 0, bringing warmer SAT from the ocean), which leads to a negative correlation as snowfall (and thus SMB) is enhanced on this windward side. As the moisture-depleted air masses flow back down on the leeward side, the temperature increases (MSWD > 0 and SAT increase further) due to the Foehn effect, thus leading to a positive correlation on this leeward side.

The Trans-Antarctic Mountains represent very steep topography but this MSWD-SAT positive/negative polarity is also observed in regions with less dramatic topography. Berkner Island (BI on Fig.2) shows a very distinctive negative MSWD-SAT correlation on its eastern side and positive on its western side, which matches the dominant westward wind direction here. Zooming in on the DML coast (Fig.4), each ice promontory and ice rise shows a distinctive east-west MSWD-SAT correlation, with the positive correlation found on the west sides, matching the dominant year-round westward wind direction in the area (see supplementary Fig.S9).

After examining the link with SAT, we will now focus on the link with SMB. We see that the areas with a low SMB-SAT correlation tend to have a significantly less negative/weak MSWD-SMB correlation. These areas correspond to (1) areas that are leeward of surface topography as dicussed above or (2) areas where katabatic winds are especially strong. For case (1), we observe that the MSWD-SMB correlation weakens or becomes positive on the leeward side of the coastal ice promontories (Fig.5). To explain this, we have to first describe average conditions. In coastal areas, synoptic air masses carry moist air across the surface topography, releasing a significant fraction of their moisture as snow on the windward side, creating a dry accumulation shadow on the leeward side. This has been observed by Lenaerts et al. (2014) for the ice rises of the DML coast. Small-scale accumulation asymmetries across ice rises have also been observed in other regions (King et al., 2004; Morse et al., 1998) and can occur on larger scales, such as across ice divides (Urbini et al., 2008) or the Trans-Antarctic Mountains (Datta

https://doi.org/10.5194/tc-2020-36
Preprint. Discussion started: 11 February 2020

et al., 2018). Stronger winds will affect this accumulation asymmetry by bringing more moisture and therefore more snow on the windward side, while the leeward side will either remain dry, or begin accumulating more snow if wind speeds allow for redistribution (Frezzotti et al., 2004). In the presence of strong winds, the MSWD-SMB correlation will therefore be strongly negative on the windward sides of ice topography and become weaker or increase on the leeward sides. This is particularly visible over the ice promontories and ice rises on Fig.5 (bottom panel) where the western sides of these ice promontories and ice rises correspond to the leeward sides based on the dominant year-round winds for the area (see Fig.S9).

Now considering case (2), winds blowing from the continent interior towards the coast are of moderate strength and tend to flow at some angle to the steepest slope when they initiate near the center of the ice sheet, carrying cold dry air from the interior (Parish and Bromwich, 1987). However, when slopes become sufficiently steep, these winds can pick up a lot of speed and blow almost directly down-slope, forming a katabatic wind regime (Parish and Bromwich, 1987). Katabatic winds transport cold dense air down-slope which can cause widespread erosion of the snow-pack through surface friction. They can also cause a warming of the SAT locally at the grounding lines through increased turbulence where the surface slope breaks from steep ice to flat shelf ice (Lenaerts et al., 2017). We therefore expect that the areas regularly under the influence of strong katabatic winds will show a weaker MSWD-SMB correlation due to the episodic but persistent reduction in their SMB through wind scouring (Agosta et al., 2019). In those areas, katabatic winds reduce SMB sufficiently to overwhelm the original synoptic SMB signal (Scambos et al., 2012; Das et al., 2013). The turbulence-induced warming effect of these katabatic winds is also observed in the MSWD-SAT correlation. The Amery Embayment (marked on Fig.2) is a good example of a region where katabatic winds are highly present. As a result, the Amery Embayment is associated with very strong sublimation rates (surface and blowing snow sublimation), lowering the local SMB and creating areas of exposed blue ice (Markov et al., 2019) with a reduced albedo in summer (so high SATs). The Amery Embayment shows therefore a weaker MSWD-SMB correlation and a very positive MSWD-SAT correlation, both spatially more extensive on the eastern side of the Amery Embayment where katabatics reach further inland and flow directly down-slope (Parish and Bromwich, 1987). The Byrd Glacier outlet into the Ross Ice Shelf (marked on Fig.2) is also an area where katabatics are strong enough to affect SMB significantly (Ligtenberg et al., 2014; Bromwich, 1989; Parish and Bromwich, 1987). Due to channeling of the wind and high sublimation/erosion of the surface, most of Byrd Glacier is completely covered with blue ice (SMB = 0 or negative), which agrees with our observed weak MSWD-SMB correlation. In other cases, large-scale air mass input could be sufficiently high that katabatic winds do not affect the deposited surface snow enough to break the large-scale link between SMB and SAT. For example, Adélie Land (marked on Fig.2), known for its record-high katabatics (van den Broeke et al., 2002), does not display particularly weak MSWD-SMB or MSWD-SAT correlations in RACMO2.3 results.

If we now combine the effects of the wind on SAT and SMB, we see that the areas that have a low SMB-SAT correlation (outlined by magenta lines on Fig.2) correspond to a generally positive MSWD-SAT correlation (Fig.4) and weak MSWD-SMB correlation (Fig5). The winds, Foehn or katabatics, affect local SAT and SMB in those areas but not to the same extent. The synoptic signal consisting of warm and moist air input is therefore overwhelmed by wind-induced local SAT or SMB changes, resulting in a weak SMB-SAT correlation. Interestingly, we note that the ice rises present on the ice shelves themselves along the DML coast on Fig.3 do not show a weak SMB-SAT correlation. However, they show both positive MSWD-SMB and

https://doi.org/10.5194/tc-2020-36
Preprint. Discussion started: 11 February 2020

MSWD-SAT correlations on their leeward sides, both negative MSWD-SMB and MSWD-SAT correlations on their windward sides. Perhaps here snowfall input from further north is so high that it dominates the SMB and SAT records.

3.1.3 Spatial-scale dependence of the modelled SAT-SMB correlation

To further analyse the spatial scale dependence of the SAT-SMB correlation, we smooth the RACMO05 SMB and SAT fields over a step-wise increasing grid spacing, going up to 27.5 km. We calculate the correlation between SMB and SAT for each spatial resolutions (Fig.6). We see that spatial scaling has little effect on the SMB-SAT correlation in the model, whose average value remains between 0.48-0.49. Similarly, the areas where the SMB-SAT correlation was already weak do not change spatially, and remain co-located with the areas that have a weak SMB-SAT correlation at the 27 km scale (shown as dashed black lines). In conclusion, based on the models, the link between SAT and SMB is positive, and valid at all spatial scales, with the exception of areas where wind-induced processes sabotage the link locally.

3.2 Strength of the SMB-SAT link in the ice core data

Now that we have a better understanding from the models, let us look at the in-situ measurements of SMB, SAT and δ^{18}O.

Because ice cores provide δ^{18}O and not SAT directly, we first examine the correlation between δ^{18}O and SMB in the models to compare to the ice core records. The iGCM simulations give a δ^{18}O-SMB continent-wide average correlation of 0.45$\pm$0.12 over 1871–2000 AD (see Fig.1, panel a), compared to the average SMB-SAT correlation of 0.57$\pm$0.10 for the same time interval (Fig.1, panel c). We thus draw the same conclusions at the regional scale as Dalaiden et al. (2019) at the continental scale: the SMB-SAT correlation is stronger than the δ^{18}O-SMB correlation at the regional scale, with a difference on the order of ~0.1.

We then calculate the correlation between δ^{18}O-SMB and SMB-SAT for the ice cores, using the Nicolas and Bromwich (2014) compilation for SAT measurements. We showed earlier that the timescale used does not affect our conclusions in terms of correlation (see Fig.1). Therefore we can compare SMB-SAT correlations over different time intervals between the models and the observations. We observe a weak-to-null annual correlation between SAT and SMB in the ice cores (Fig.7) with an average value of 0.09$\pm$0.18 over all the ice cores, versus a continent-wide average value of 0.57$\pm$0.10 for the iGCMs and 0.54$\pm$0.22 for RACMO27. The same is true for the correlation between δ^{18}O and SMB with a continent-wide average value of 0.13$\pm$0.25 (5-yearly and over 1871–2010 AD). We note no observable difference in the correlation between SAT-SMB and δ^{18}O-SMB in the ice core records, as opposed to in the models.

3.3 Can our improved understanding of processes at regional scales help to explain why the SMB-SAT link measured in ice cores is different to the link as estimated in models?

We list six potential reasons why ice cores might show a weaker relationship between SMB and δ^{18}O or SMB and SAT than the models. (1) First, we argue that the difference in correlation between the models and the observations could arise in the representation of large scale processes in the models. In other words, the models (iGCMs and RCMs alike) may not represent

https://doi.org/10.5194/tc-2020-36
Preprint. Discussion started: 11 February 2020

the reality well enough because they are missing an important dynamic process, process that acts to weaken the correlation between SMB and SAT. However, we argue that this is unlikely since the iGCM and RACMO2.3 simulations agree despite their different fundamental representations of the physics at work and different resolutions. (2) A second hypothesis is that the models do not represent processes well enough at the scale of a few 10s of kilometers. 5.5 km, the RACMO2.3 spatial scale, is a spatial resolution that is still too coarse to resolve small-scale SAT or SMB-modifying processes. In particular, wind redistribution has been shown to be under-estimated in the polar-focussed RCMs (Agosta et al., 2019). Turton et al. (2017) have shown that a spatial resolution of 1.5 km is required to simulate Foehn flow accurately over the AP. In addition, we also know from observations that a lot of local-scale snow redistribution effects occur to form sastrugi, dunes, etc, which are not resolved in simulations at the 5.5 km scale (Ligtenberg et al., 2014).

(3) On the data side, we know that the Nicolas and Bromwich (2014) SAT data set is not representative of the entire AIS. With only 15 data points for the entire AIS, mostly located around the coast, this data set has a strong coastal-signal bias (see Nicolas and Bromwich (2014) supplementary material for the weather station distribution). We have shown in Fig.2 that the coastal regions correspond to weaker SMB-SAT correlations. However, it does not explain why the δ^{18}O-SMB correlation is also weak. (4) Also on the data side, the ice cores might contain a noisy record of SMB and δ^{18}O, therefore reducing the measured correlation between the two. We have to keep in mind that ice cores are point measurements on the ice sheet, with a surface area of ~31 cm^2. The ice cores are affected both by (a) measurement errors due to depth, density and age uncertainties (Parrenin et al., 2012) and (b) surface wind processes which act to redistribute the snow at the surface and therefore reduce or increase SMB very locally (e.g. ice crests, sastrugi, ice crusts, etc) or on large areas (e.g. dune fields, Das et al., 2013). This local noise, sampled in the ice core records, might get averaged out at the 5.5 km scale in models. A large number of ice cores might help reduce the noise contained in individual records, if this noise is random. However, estimating this may be hampered by the relatively low number of historical ice core records (53 ice cores were used to calculate the SMB-SAT and SMB-δ^{18}O correlations using the Stenni et al. (2017) and Thomas et al. (2017) compilations), as discussed below. (5) In addition, many of the ice cores retrieved so far from the AIS, and used in the Stenni et al. (2017) and Thomas et al. (2017) compilations, are clustered in the coastal areas, with a higher sampling in West Antarctica than in East Antarctica. This implies that the SMB-SAT correlation calculated based on these ice core compilations is likely not representative of the continent-wide, or even regional, SMB-SAT correlation. However, it cannot explain the discrepancy with the model-derived correlations as most of the ice cores used are located where the models predict a positive SMB-SAT correlation (outlined grey shading on Fig.7). (6) Finally, we examine the correlation between SMB and SAT on annual timescales, but we know that SMB (snowfall in this case) is brought to the AIS in very episodic ways (atmospheric rivers, etc, Gorodetskaya et al., 2014). Using annual values might not be representative of the conditions during accumulation. Turner et al. (2019) show that more than 70% of the annual accumulation consists of extreme events that have a very short duration (one or more consecutive days).

To see whether the lack of correlation between SMB and SAT in ice cores versus models is due to the presence of local random noise in the ice core records, we aggregate ice cores onto a regularly spaced grid, similarly to how we smoothed the RACMO2.3 data previously (see Fig.6). Since there are few ice cores (53), we use the RACMO27 model grid and average the ice core records every four grid points, i.e. we aggregate ice cores on a 108 x 108 km regular grid. If the lack of correlation

https://doi.org/10.5194/tc-2020-36
Preprint. Discussion started: 11 February 2020

between SMB and SAT is due to random noise that operates below the RACMO5 spatial scale, we should see an increase in the SMB-SAT correlation using the aggregated climate records. Of course, we will only see an increase in the SMB-SAT with ice core aggregation if we have enough ice cores. We observe that both the SMB-SAT and the δ^{18}O-SMB correlations remain at 0.09 and 0.13 respectively. If we average records every eight grid points (216 x 216 km grid), the SMB-SAT correlation increases up to 0.12 from 0.09 previously, while the δ^{18}O-SMB correlation increases to 0.16 from 0.13 previously (see Fig.8). This is more consistent with what we concluded from the models, and suggests that part of the discrepancy between ice cores and models is in fact due to noise at the ice core level. The correlation remains low compared to the models, however.

We repeat the scaling experiment but increase further the distance over which we aggregate the ice core records, from every four RACMO27 grid points step-wise up to every 24 RACMO27 grid points (i.e. 648 x 648 km grid). We only retain grid points that aggregate five or more ice cores to have sufficient averaging of the ice core records. For each retained grid point, we calculate (1) the mean of the SMB-SAT correlation of each individual ice core aggregated (= "individual mean") and (2) the correlation of the averaged SMB and SAT from the aggregated ice cores (= "aggregate value"). Due to the scarcity of ice core measurements, few grid points satisfy our condition of five or more ice cores (only three grid points contain at least five ice cores at the 648 x 648 km grid resolution). Results are shown in Fig.9. Two conclusions emerge from this scaling experiment: (1) the aggregate correlation is generally higher than the individual mean correlation (and always higher if we use at least ten ice cores), (2) this is true at all spatial scales. Per grid point, averaging the climate signals in the ice core records before calculating the correlations (i.e. the aggregate value) increases the ice core SMB-SAT correlations by ~0.1-0.2, reaching a correlation up to 0.2-0.3 if at least 10 ice cores are aggregated.

For comparison, we calculate the individual mean and the aggregate value of the SMB-SAT correlation for the RACMO27-simulated SMB and SAT fields, for the same grid points as for the ice cores (also shown on Fig.9 in grey). This to compare the model-derived and ice core-derived correlations locally. Similarly to the ice cores, the aggregate value is always higher than the individual mean for the RACMO27-derived SMB-SAT correlation.

We note there is a weak but positive trend in the ice core-based results, where increasing the number of records averaged over increases the SMB-SAT correlation. The SMB-SAT correlation is consistently lower for the ice cores than for the models, aggregate and individual mean values alike. The gap between the models and the ice cores reduces with spatial scaling but remains large. We conclude that there is some random local noise in the ice core records that can be removed by simple averaging over multiple cores. Aggregating the ice core records increases the signal-to-noise ratio of their climate records. However, the increase in correlation is low. Models may overestimate the correlation at scale of tens of kms but it is also likely that we are not able to increase the signal-to-noise ratio sufficiently in the records and reach the obtained model correlation. Another explanation is that we are not able to quantify some systematic processes and effects that occur between the model scale and the ice core scale that must be taken into account. In that case, retrieving multiple cores in different regions is maybe not the most appropriate option (if only for practical reasons). We need to better understand the spatial representativity of the ice core records. The sparse distribution of the ice core measurements impacts their representativity for the whole ice sheet. Frezzotti et al. (2004) had calculated at the time that the total number of accumulation data point measurements (including stakes and non-ice core measurements) reached 1,860 for the entire AIS, representing one data point every 6,500 km^2.

https://doi.org/10.5194/tc-2020-36
Preprint. Discussion started: 11 February 2020

We know that the surface of the ice sheet is incredibly rough at the scale of an ice core which will greatly influence the climate records retrieved through wind-topography dynamic feedbacks (Frezzotti et al., 2002a). Furthermore, the location of an ice core is often chosen based on surface topography and surface features: smooth surface, absence of dunes or surface erosion, top of a dome or of an ice rise, etc. However, dynamic processes, although not acting today, might have been active in the past, as evidenced from ice-penetrating radar data (e.g. Arcone et al., 2012b; Cavitte et al., 2016; Frezzotti et al., 2002a), and therefore can have affected the ice core records examined.

Both the snow accumulation and the isotopic signal recorded in ice cores contain a signature of the post-depositional processes occurring at the surface and the intermittency of precipitation. Extreme precipitation events can explain 70% of the variance of annual precipitation (Turner et al., 2019), for which the greatest contribution occurs in coastal areas. This would suggest that the ice core climatic signal contains only a snapshot of conditions, rather than a continuous record. This is especially important in the stable water isotope records, which are already precipitation biased (only recording temperature during periods of snowfall) and further complicated by isotopic diffusion. Based solely on physical processes, the local noise in some regions overwhelms the climatic signal at timescales of less than 1000 years (Casado et al., 2019). Using only high accumulation sites (> 0.5 m yr^{-1} at least once over the 1958–2010 AD interval), the resulting SMB-SAT ice core correlation average over the continent increases from 0.09 ± 0.18 initially to 0.28 ± 0.25. Keeping only high accumulation sites seems thus to reduce the impact of post-depositional effects. We are however left with a 13-ice core compilation, with a strong spatial bias towards West Antarctica and the AP.

4 Conclusions

We have shown that there is a positive correlation between SMB and SAT over the AIS, particularly in the interior of the ice sheet, and between SMB and δ^{18}O although it is weaker than for SMB and SAT. This confirms what has already been shown at the continental scale (Dalaiden et al., 2019). The main source of accumulation over the AIS comes from further north through large-scale atmospheric circulation that carries warm moist air to the continent (Gorodetskaya et al., 2014; Wang et al., 2019), therefore resulting in the overall positive SMB-SAT correlation observed. There are a few areas of the AIS where the SMB-SAT correlation does not hold strong, generally found in the coastal areas. These are areas where wind-driven processes act on the SMB or SAT locally, through Foehn and katabatic warming and erosion. If the winds are sufficiently strong, they overwhelm the synoptic-scale inputs that induce the positive SMB-SAT and SMB-δ^{18}O correlations.

In models, the SMB-SAT correlation does not seem to be strongly scale-dependent, which we expect due to the lack of noise in models in general. However, the spatial resolution of the models does influence whether we can resolve small-scale topography where wind processes have a dominant influence (e.g. individual ice promontories) and therefore detect a local reduction in the SMB-SAT link. At the ice core scale, we have shown that the correlation between SMB and SAT is much weaker (even though the ice cores are located in regions with a high model SMB-SAT correlation), corroborating the observations made at the continental scale by Dalaiden et al. (2019). Averaging ice core records in close spatial proximity improves their SMB-SAT correlation, probably due to random noise averaging. Such an increase of the SMB-SAT correlation with averaging indicates

https://doi.org/10.5194/tc-2020-36
Preprint. Discussion started: 11 February 2020

that the processes detected in the models can also be detected in ice core data, even if the strength of the SMB-SAT link remains lower than in the models. However, in addition to this random noise, ice cores might be affected by a number of local processes that perturb the measured correlation between SMB and SAT systematically and cannot be removed through simple averaging. Choosing only high accumulation ice core sites help improve the measured correlation between SMB and SAT but reduces the number of ice cores left to a handful.

This implies that we must correct for the local processes present in each ice core record so that their spatial representativity is closer to that of the models, or models must increase their spatial resolution to better resolve wind effects, to improve our confidence in using SMB as a direct proxy for SAT over the entire AIS.

https://doi.org/10.5194/tc-2020-36
Preprint. Discussion started: 11 February 2020

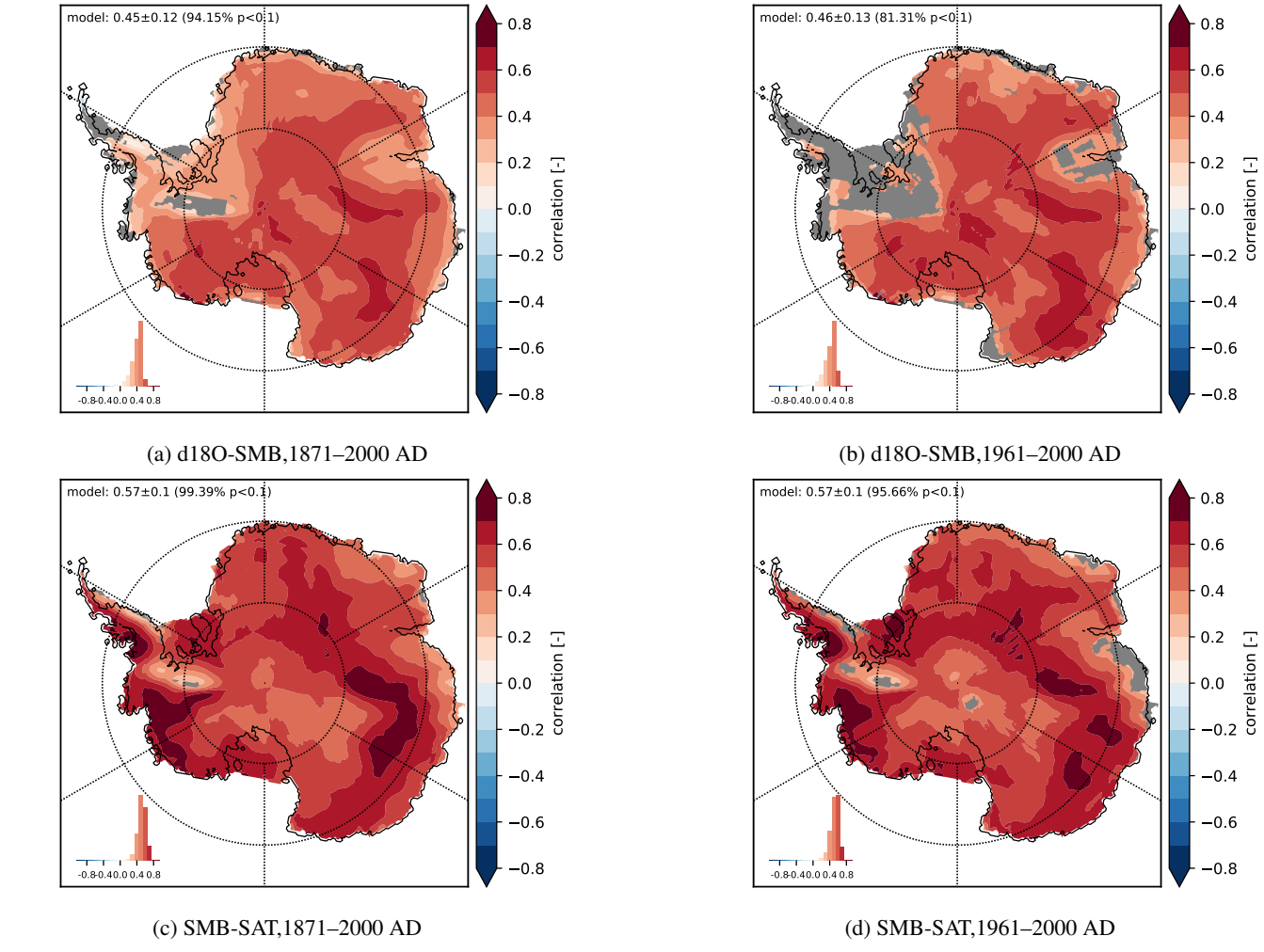

(a) d18O-SMB,1871–2000 AD

(b) d18O-SMB,1961–2000 AD

(c) SMB-SAT,1871–2000 AD

(d) SMB-SAT,1961–2000 AD

Figure 1. Annual correlation averaged over all the isotopic GCMs between (a) δ^{18}O and SMB over 1871–2000 AD and (b) 1961–2000 AD; (c) between SMB and SAT over 1871–2000 AD and (d) 1961–2000 AD. Statistically insignificant areas ($p > 0.1$) are hashed in grey . The histogram displays the distribution of correlation values. Continent-wide correlation mean, standard deviation and percentage of model area with $p < 0.1$ averaged over all 4 isotopic GCMs are provided on each panel.

https://doi.org/10.5194/tc-2020-36
Preprint. Discussion started: 11 February 2020

The Cryosphere
Discussions
Open Access
EGU

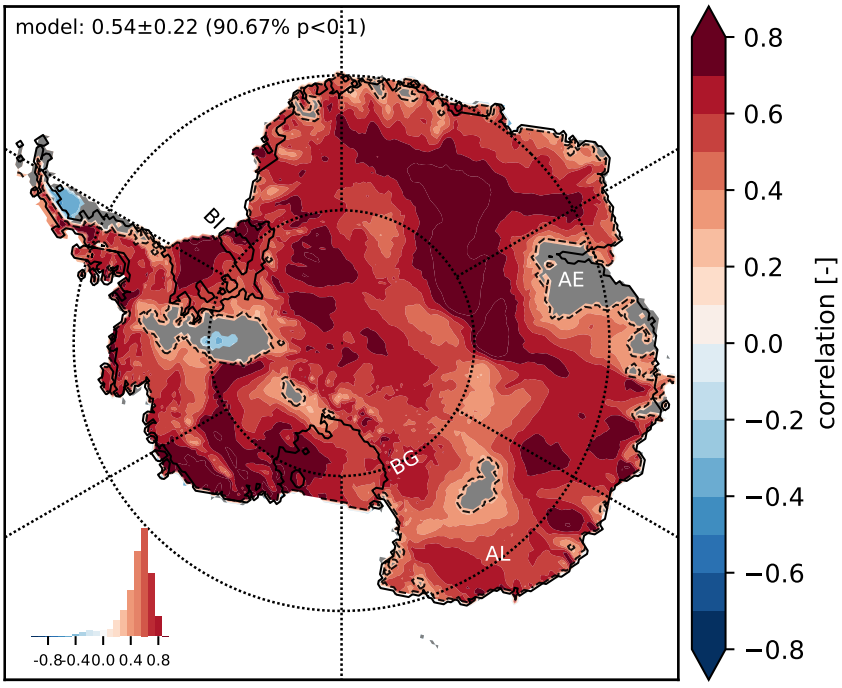

Figure 2. Annual correlation between SMB and SAT for RACMO2.3 over 1979–2016 AD at the 27 km spatial resolution. Statistically insignificant areas ($p > 0.1$) are in grey, outlined with a dashed black line. The histogram displays the distribution of correlation values. Continent-wide correlation mean, standard deviation and percentage of model area with $p < 0.1$ are provided on the figure. Specific locations mentioned are annotated on the figure: 'BI', Berkner Island - 'BG', Byrd Glacier - 'AE', Amery Embayment - 'AL', Adélie Land

https://doi.org/10.5194/tc-2020-36
Preprint. Discussion started: 11 February 2020

The Cryosphere Discussions
Open Access
EGU

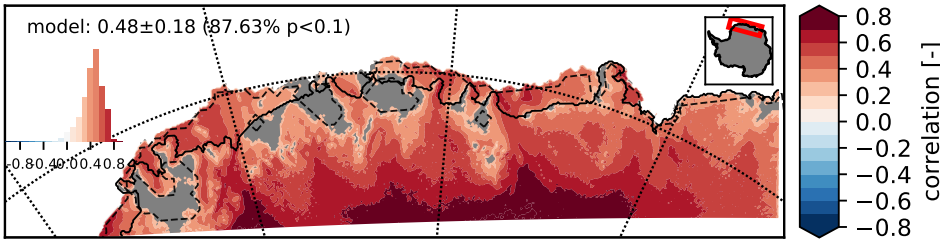

(a) RACMO5

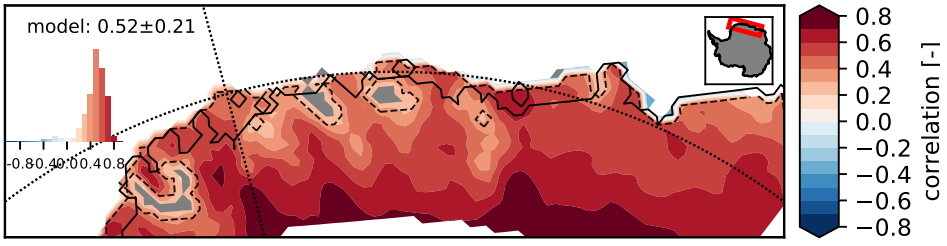

(b) RACMO27

Figure 3. Annual correlation between SMB and SAT for RACMO2.3 over 1979–2016 AD at the (a) 5.5 km and (b) 27 km spatial resolution for Dronning Maud Land. Statistically insignificant areas ($p > 0.1$) are in grey. The dashed black lines on both panels correspond to the areas with $p > 0.1$ at the 27 km resolution. The histogram displays the distribution of correlation values. Region-wide correlation mean, standard deviation and percentage of model area with $p < 0.1$ are provided on each panel.

https://doi.org/10.5194/tc-2020-36
Preprint. Discussion started: 11 February 2020

The Cryosphere
Discussions
Open Access
EGU

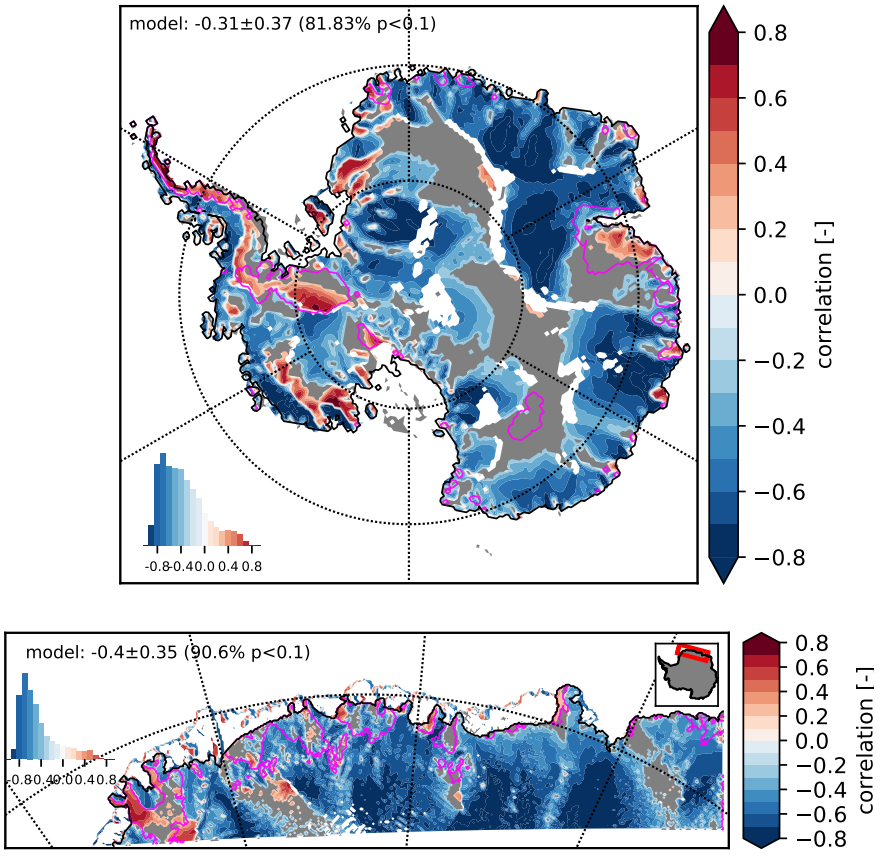

Figure 4. Annual correlation between MSWD and SAT using (top) RACMO27 and (bottom) RACMO5 simulations over 1979–2016 AD. Statistically insignificant areas ($p > 0.1$) are in grey. Areas with a slope smaller than 0.1% are removed and appear in white. Magenta lines outline the areas that have a weak SMB-SAT correlation in Fig.2. The histogram displays the distribution of correlation values. Continent- or region-wide correlation mean, standard deviation and percentage of model area with $p < 0.1$ are provided on each panel.

https://doi.org/10.5194/tc-2020-36
Preprint. Discussion started: 11 February 2020

The Cryosphere
Discussions
Open Access
EGU

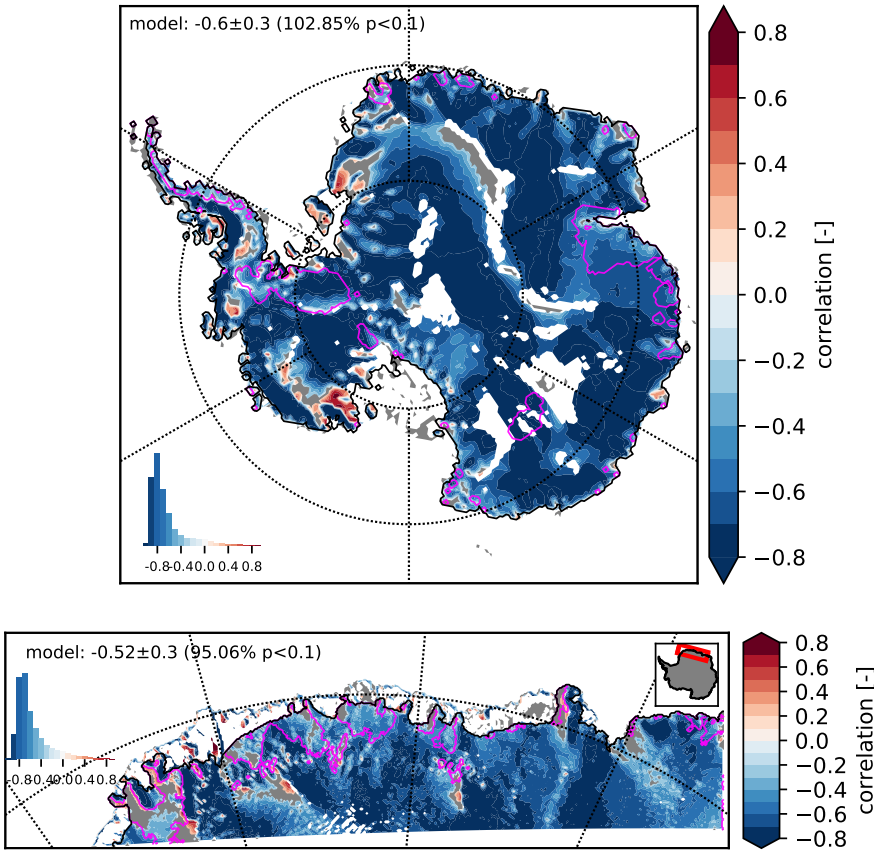

Figure 5. Annual correlation between MSWD and SMB using (top) RACMO27 and (bottom) RACMO5 simulations over 1979–2016 AD. Statistically insignificant areas ($p > 0.1$) are in grey. Areas with a slope smaller than 0.1% are removed and appear in white. Magenta lines outline the areas that have a weak SMB-SAT correlation in Fig.2. The histogram displays the distribution of correlation values. Continent- or region-wide correlation mean, standard deviation and percentage of model area with $p < 0.1$ are provided on each panel.

https://doi.org/10.5194/tc-2020-36
Preprint. Discussion started: 11 February 2020

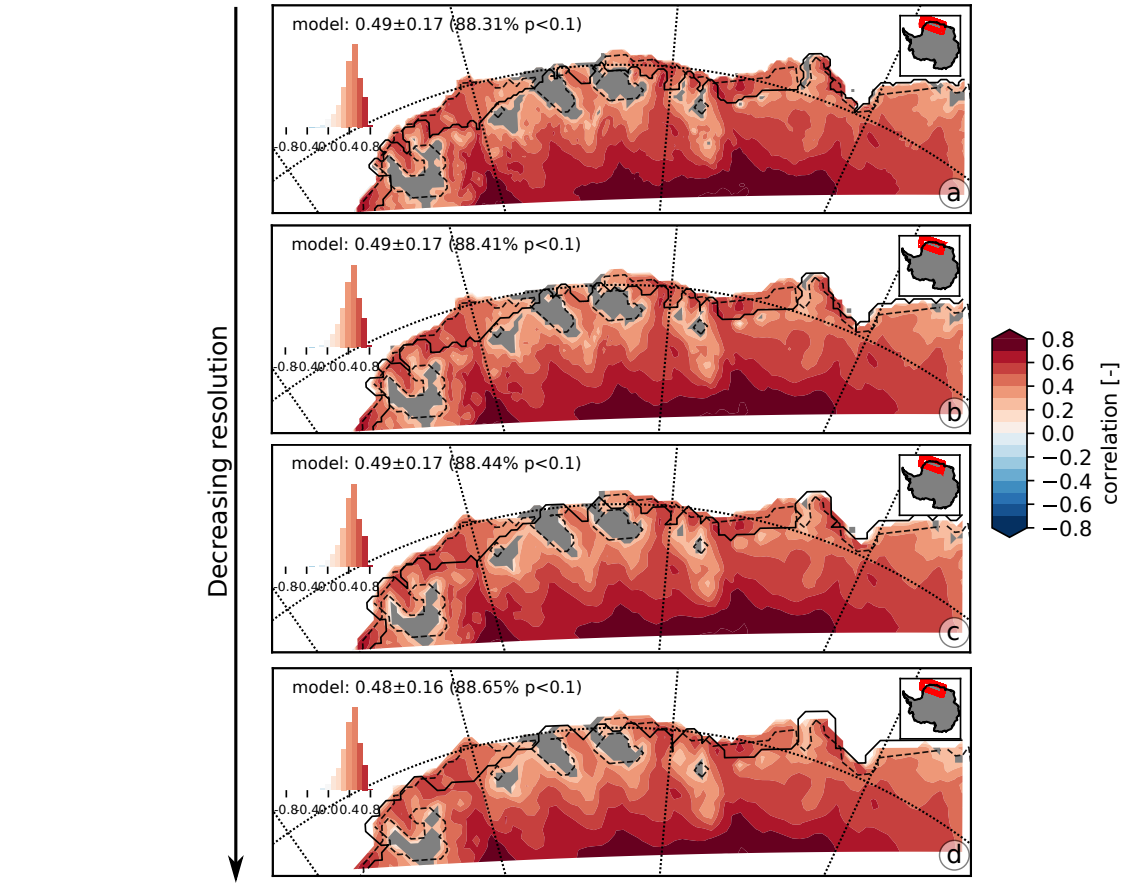

Figure 6. Annual correlation between SMB and SAT for RACMO05 simulations over increasing grid scalings from top to bottom: (a) 11 km, (b) 16.5 km, (c) 22 km and (d) 27.5 km over 1979–2016 AD. Statistically insignificant areas ($p > 0.1$) for each resolution are hashed in grey. A dashed black line outlines the areas with a low SAT-SMB correlation from Fig.2 for comparison. The histogram displays the distribution of correlation values for each panel. Region-wide correlation mean, standard deviation and percentage of model area with $p < 0.1$ are provided on each panel.

https://doi.org/10.5194/tc-2020-36
Preprint. Discussion started: 11 February 2020

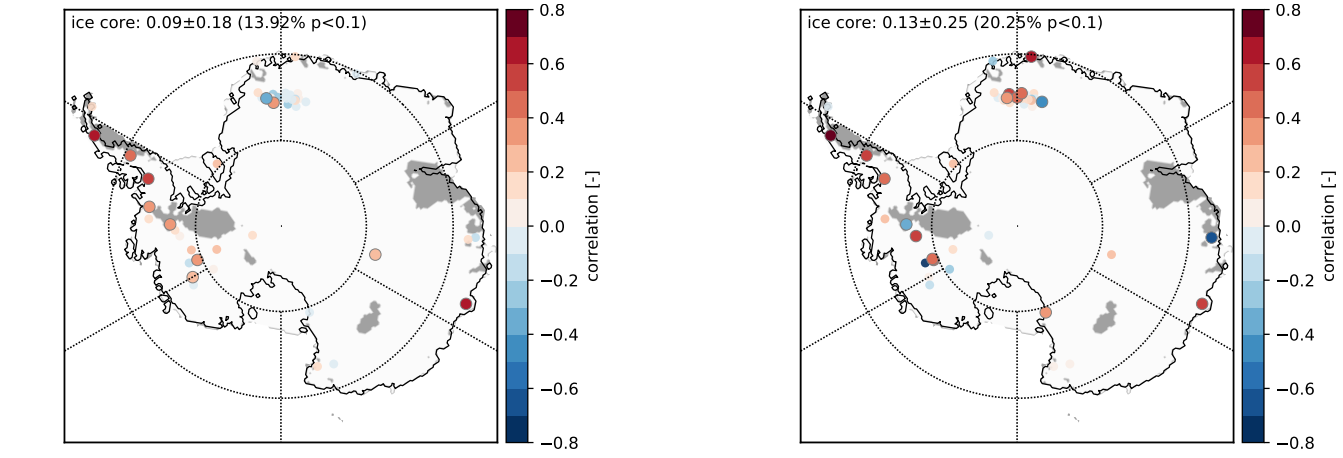

(a) SMB-SAT

(b) δ^{18}O-SMB

Figure 7. Ice core correlations (a) annually for SMB–SAT over 1958–2010 AD and (b) 5-yearly for δ^{18}O-SMB over 1871–2010 AD. Large dots indicate that the correlation value is significantive, smaller dots indicate a p-value > 0.1. Statistically insignificant areas (p > 0.1) of the RACMO27 SMB-SAT correlation are hashed in grey for reference. The average correlation, standard deviation and percentage over all the ice cores is provided on each panel.

https://doi.org/10.5194/tc-2020-36
Preprint. Discussion started: 11 February 2020

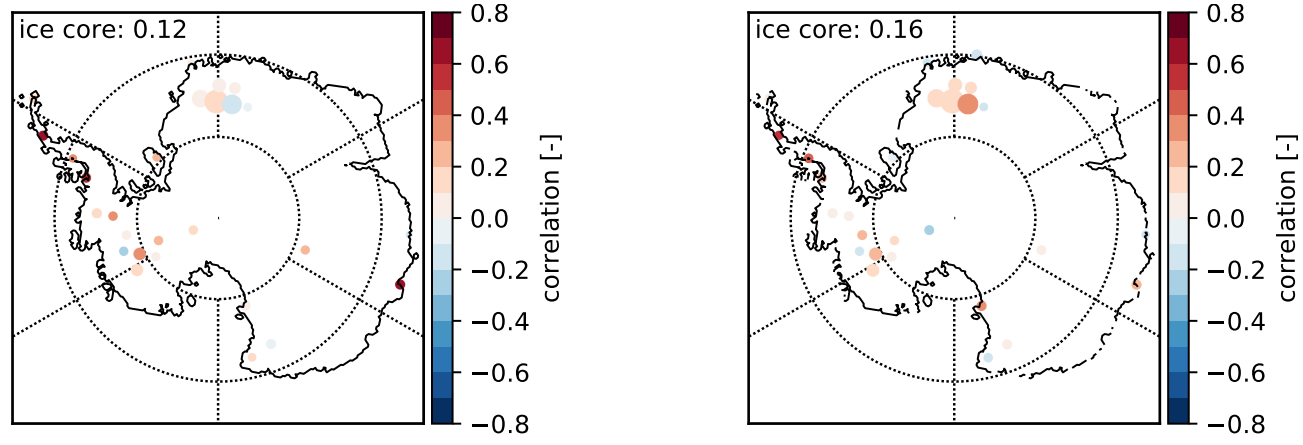

(a) SMB-SAT

(b) δ^{18}O-SMB

Figure 8. Aggregated ice core correlations on a 216 x 216 km grid for (a) SMB-SAT annually over 1958–2010 AD and (b) δ^{18}O-SMB 5-yearly over 1871–2010 AD. The mean correlation over all the ice cores is provided on each panel.

https://doi.org/10.5194/tc-2020-36
Preprint. Discussion started: 11 February 2020

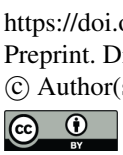

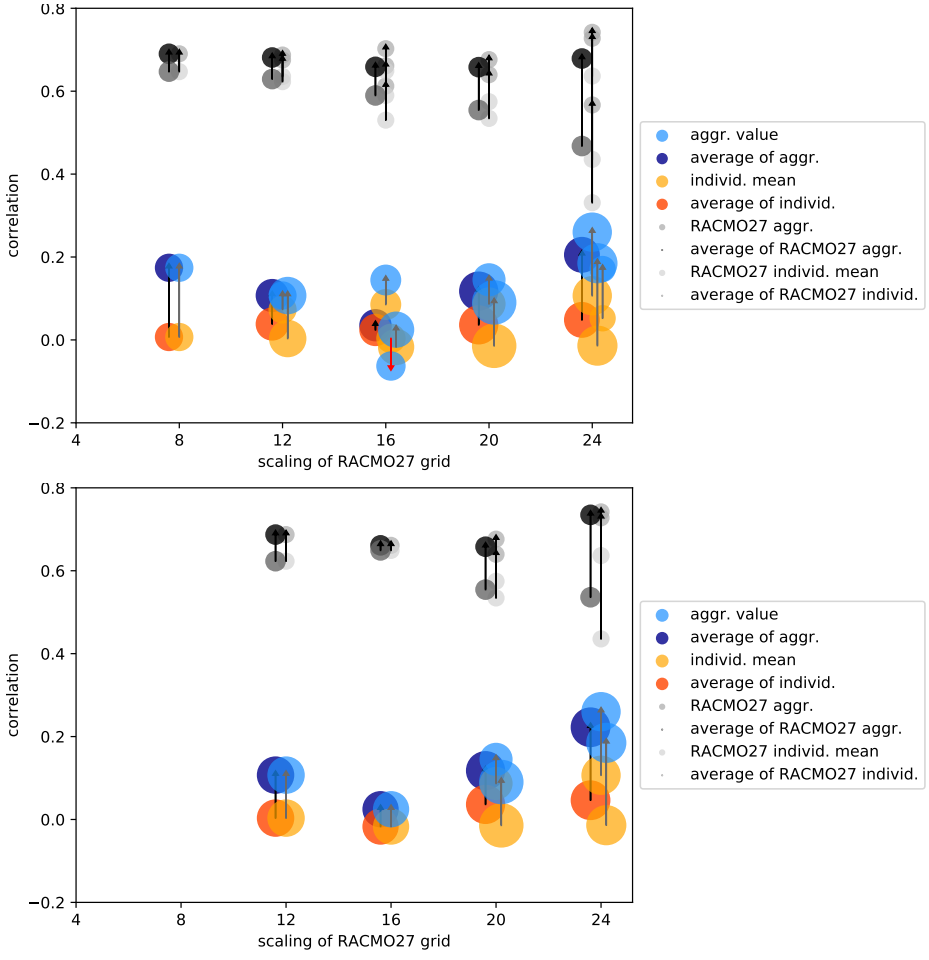

Figure 9. SMB-SAT correlation as a function of grid spacing for the aggregated records versus mean of the individual correlations for the ice cores (blues and yellows, respectively) and RACMO27 simulations (in dark and light grey, respectively). The size of the colored dots is a function of the number of ice cores aggregated for that grid point. Only grid points with at least (top) five and (bottom) ten ice cores are kept. Correlations are over the 1958–2010 AD time interval.

Data availability. RACMO2.3 simulations are available by request to J.T.M. Lenaerts (jan.lenaerts@colorado.edu); CMIP5 simulations are available at http://pcmdi9.llnl.gov; iHadCM3 simulations are available by request to Max Holloway (max.holloway@sams.ac.uk); ECHAM5-wiso simulations are available at https://doi.org/10.5281/zenodo.1249604; ECHAM5/MPI-OM simulations are available by request to Jesper Sjolte (jesper.sjolte@geol.lu.se). The δ^{18}O Stenni et al. (2017) compilation is available at https://www.ncdc.noaa.gov/paleo-search/study/22589, the SMB Thomas et al. (2017) compilation is available by a request to Elizabeth R. Thomas (lith@bas.ac.uk), the SAT Nicolas and Bromwich (2014) compilation is available at http://polarmet.osu.edu/datasets.

https://doi.org/10.5194/tc-2020-36
Preprint. Discussion started: 11 February 2020

Author contributions. MGPC and HG designed the experiments and MGPC carried them out. QD provided analysis support, JTML provided RACMO support, ERT provided ice core support. MGPC prepared the manuscript with contributions from all co-authors.

Competing interests. The authors declare no competing interests.

Acknowledgements. We would like to thank Melchior Van Wessem for the RACMO2.3 model outputs. We acknowledge the World Climate Research Programme Working Group on Coupled Modelling,responsible for CMIP. This work was supported by the Belgian Research Action through Interdisciplinary Networks (BRAIN-be) from Belgian Science Policy Office in the framework of the project "East Antarctic surface mass balance in the Anthropocene: observations and multiscale modelling (Mass2Ant)" (Contrat n° BR/165/A2/Mass2Ant). Hugues Goosse is the research director within the F.R.S.-FNRS.

https://doi.org/10.5194/tc-2020-36
Preprint. Discussion started: 11 February 2020

References

Agosta, C., Amory, C., Kittel, C., Orsi, A., Favier, V., Gallée, H., van den Broeke, M. R., Lenaerts, J., van Wessem, J. M., van de Berg, W. J., et al.: Estimation of the Antarctic surface mass balance using the regional climate model MAR (1979-2015) and identification of dominant processes, Cryosphere, 13, 281–296, 2019.

Arcone, S. A., Jacobel, R., and Hamilton, G.: Unconformable stratigraphy in East Antarctica: Part I. Large firn cosets, recrystallized growth, and model evidence for intensified accumulation, Journal of Glaciology, 58, 240–252, https://doi.org/10.3189/2012JoJ11J044, 2012a.

Arcone, S. A., Jacobel, R., and Hamilton, G.: Unconformable stratigraphy in East Antarctica: Part II. Englacial cosets and recrystallized layers, Journal of Glaciology, 58, 253–264, https://doi.org/10.3189/2012JoG11J045, 2012b.

Ball, F. K.: The Katabatic Winds of Adélie Land and King George V Land, Tellus, 9, 201–208, https://doi.org/10.1111/j.2153-3490.1957.tb01874.x, https://onlinelibrary.wiley.com/doi/abs/10.1111/j.2153-3490.1957.tb01874.x, 1957.

Black, H. and Budd, W.: Accumulation in the region of Wilkes, Wilkes Land, Antarctica, Journal of Glaciology, 5, 3–15, 1964.

Brady, E., Stevenson, S., Bailey, D., Liu, Z., Noone, D., Nusbaumer, J., Otto-Bliesner, B., Tabor, C., Tomas, R., Wong, T., et al.: The connected isotopic water cycle in the Community Earth System Model version 1, Journal of Advances in Modeling Earth Systems, 2019.

Bromwich, D. H.: Satellite analyses of Antarctic katabatic wind behavior, Bulletin of the American meteorological society, 70, 738–749, 1989.

Bromwich, D. H. and Liu, Z.: An observational study of the katabatic wind confluence zone near Siple Coast, West Antarctica, Monthly weather review, 124, 462–477, 1996.

Budd, W.: An analysis of the relation between the surface and bedrock profiles of ice caps, Journal of Glaciology, 10, 197–209, 1971.

Casado, M., Münch, T., and Laepple, T.: Climatic information archived in ice cores: impact of intermittency and diffusion on the recorded isotopic signal in Antarctica, Climate of the Past Discussions, 2019, 1–27, https://doi.org/10.5194/cp-2019-134, https://www.clim-past-discuss.net/cp-2019-134/, 2019.

Cavitte, M. G., Blankenship, D. D., Young, D. A., Schroeder, D. M., Parrenin, F., Lemeur, E., Macgregor, J. A., and Siegert, M. J.: Deep radiostratigraphy of the East Antarctic plateau: connecting the Dome C and Vostok ice core sites, Journal of Glaciology, 62, 323–334, 2016.

Dalaiden, Q., Goosse, H., Klein, F., Lenaerts, J. T. M., Holloway, M., Sime, L., and Thomas, E. R.: Surface Mass Balance of the Antarctic Ice Sheet and its link with surface temperature change in model simulations and reconstructions, The Cryosphere Discussions, 2019, 1–29, https://doi.org/10.5194/tc-2019-111, https://www.the-cryosphere-discuss.net/tc-2019-111/, 2019.

Das, I., Bell, R. E., Scambos, T. A., Wolovick, M., Creyts, T. T., Studinger, M., Frearson, N., Nicolas, J. P., Lenaerts, J. T., and van den Broeke, M. R.: Influence of persistent wind scour on the surface mass balance of Antarctica, Nature Geoscience, 6, 367–371, https://doi.org/10.1038/ngeo1766, 2013.

Datta, R. T., Tedesco, M., Agosta, C., Fettweis, X., Kuipers Munneke, P., and van den Broeke, M.: Melting over the northeast Antarctic Peninsula (1999–2009): evaluation of a high-resolution regional climate model, Cryosphere (The), 12, 2901–2922, 2018.

Datta, R. T., Tedesco, M., Fettweis, X., Agosta, C., Lhermitte, S., Lenaerts, J., and Wever, N.: The Effect of Foehn-Induced Surface Melt on Firn Evolution Over the Northeast Antarctic Peninsula, Geophysical Research Letters, 46, 2019.

Dattler, M. E., Lenaerts, J. T. M., and Medley, B.: Significant Spatial Variability in Radar-Derived West Antarctic Accumulation Linked to Surface Winds and Topography, Geophysical Research Letters, n/a, https://doi.org/10.1029/2019GL085363, https://agupubs.onlinelibrary.wiley.com/doi/abs/10.1029/2019GL085363, 2019.

https://doi.org/10.5194/tc-2020-36
Preprint. Discussion started: 11 February 2020

ECMWF: Part IV: Physical Processes, no. 4 in IFS Documentation, ECMWF, https://www.ecmwf.int/node/9227, operational implementation 3 June 2008, 2009.

Elvidge, A. D. and Renfrew, I. A.: The causes of foehn warming in the lee of mountains, Bulletin of the American Meteorological Society, 97, 455–466, 2016.

Elvidge, A. D., Renfrew, I. A., King, J. C., Orr, A., Lachlan-Cope, T. A., Weeks, M., and Gray, S. L.: Foehn jets over the Larsen C ice shelf, Antarctica, Quarterly Journal of the Royal Meteorological Society, 141, 698–713, 2015.

Favier, V., Agosta, C., Parouty, S., Durand, G., Delaygue, G., Gallée, H., Drouet, A.-S., Trouvilliez, A., and Krinner, G.: An updated and quality controlled surface mass balance dataset for Antarctica, The Cryosphere, 7, 583–597, https://doi.org/10.5194/tc-7-583-2013, https://www.the-cryosphere.net/7/583/2013/, 2013.

Frezzotti, M., Gandolfi, S., La Marca, F., and Urbini, S.: Snow dunes and glazed surfaces in Antarctica: new field and remote-sensing data, Annals of Glaciology, 34, 81–88, 2002a.

Frezzotti, M., Gandolfi, S., and Urbini, S.: Snow megadunes in Antarctica: sedimentary structure and genesis, Journal of Geophysical Research: Atmospheres, 107, 2002b.

Frezzotti, M., Pourchet, M., Flora, O., Gandolfi, S., Gay, M., Urbini, S., Vincent, C., Becagli, S., Gragnani, R., Proposito, M., et al.: New estimations of precipitation and surface sublimation in East Antarctica from snow accumulation measurements, Climate Dynamics, 23, 803–813, 2004.

Frezzotti, M., Urbini, S., Proposito, M., Scarchilli, C., and Gandolfi, S.: Spatial and temporal variability of surface mass balance near Talos Dome, East Antarctica, Journal of Geophysical Research: Earth Surface, 112, 2007.

Frieler, K., Clark, P. U., He, F., Buizert, C., Reese, R., Ligtenberg, S. R., Van Den Broeke, M. R., Winkelmann, R., and Levermann, A.: Consistent evidence of increasing Antarctic accumulation with warming, Nature Climate Change, 5, 348–352, 2015.

Fujita, S., Holmlund, P., Andersson, I., Brown, I., Enomoto, H., Fujii, Y., Fujita, K., Fukui, K., Furukawa, T., Hansson, M., et al.: Spatial and temporal variability of snow accumulation rate on the East Antarctic ice divide between Dome Fuji and EPICA DML, The Cryosphere, 5, 1057–1081, 2011.

Gorodetskaya, I. V., Tsukernik, M., Claes, K., Ralph, M. F., Neff, W. D., and Van Lipzig, N. P. M.: The role of atmospheric rivers in anomalous snow accumulation in East Antarctica, Geophysical Research Letters, 41, 6199–6206, https://doi.org/10.1002/2014GL060881, https://agupubs.onlinelibrary.wiley.com/doi/abs/10.1002/2014GL060881, 2014.

Goursaud, S., Masson-Delmotte, V., Favier, V., Preunkert, S., Fily, M., Gallée, H., Jourdain, B., Legrand, M., Magand, O., Minster, B., et al.: A 60-year ice-core record of regional climate from Adélie Land, coastal Antarctica, The Cryosphere, 11, 343–362, 2017.

Goursaud, S., Masson-Delmotte, V., Favier, V., Preunkert, S., Legrand, M., Minster, B., and Werner, M.: Challenges associated with the climatic interpretation of water stable isotope records from a highly resolved firn core from Adélie Land, coastal Antarctica, The Cryosphere, 13, 1297–1324, https://doi.org/10.5194/tc-13-1297-2019, https://www.the-cryosphere.net/13/1297/2019/, 2019.

Grima, C., Blankenship, D. D., Young, D. A., and Schroeder, D. M.: Surface slope control on firn density at Thwaites Glacier, West Antarctica: Results from airborne radar sounding, Geophysical Research Letters, 41, 6787–6794, 2014.

Holloway, M. D., Sime, L. C., Singarayer, J. S., Tindall, J. C., Bunch, P., and Valdes, P. J.: Antarctic last interglacial isotope peak in response to sea ice retreat not ice-sheet collapse, Nature communications, 7, 12 293, 2016.

King, J., Anderson, P., Vaughan, D., Mann, G., Mobbs, S., and Vosper, S.: Wind-borne redistribution of snow across an Antarctic ice rise, Journal of Geophysical Research: Atmospheres, 109, 2004.

Klein, F., Abram, N. J., Curran, M. A. J., Goosse, H., Goursaud, S., Masson-Delmotte, V., Moy, A., Neukom, R., Orsi, A., Sjolte, J., Steiger, N., Stenni, B., and Werner, M.: Assessing the robustness of Antarctic temperature reconstructions over the past 2 millennia using pseudoproxy and data assimilation experiments, Climate of the Past, 15, 661–684, https://doi.org/10.5194/cp-15-661-2019, https://www.clim-past.net/15/661/2019/, 2019.

Lenaerts, J., Brown, J., van den Broeke, M., Matsuoka, K., Drews, R., Callens, D., Philippe, M., Gorodetskaya, I. V., Van Meijgaard, E., Tijm-Reijmer, C., et al.: High variability of climate and surface mass balance induced by Antarctic ice rises, Journal of Glaciology, 60, 1101–1110, 2014.

Lenaerts, J., Lhermitte, S., Drews, R., Ligtenberg, S., Berger, S., Helm, V., Smeets, C., Van den Broeke, M., Van De Berg, W. J., Van Meijgaard, E., et al.: Meltwater produced by wind–albedo interaction stored in an East Antarctic ice shelf, Nature climate change, 7, 58, 2017.

Lenaerts, J. T. M., van den Broeke, M. R., Déry, S. J., König-Langlo, G., Ettema, J., and Munneke, P. K.: Modelling snowdrift sublimation on an Antarctic ice shelf, The Cryosphere, 4, 179–190, https://doi.org/10.5194/tc-4-179-2010, https://www.the-cryosphere.net/4/179/2010/, 2010.

Lenaerts, J. T. M., Medley, B., van den Broeke, M. R., and Wouters, B.: Observing and Modeling Ice Sheet Surface Mass Balance, Reviews of Geophysics, 57, 376–420, https://doi.org/10.1029/2018RG000622, https://agupubs.onlinelibrary.wiley.com/doi/abs/10.1029/2018RG000622, 2019.

Ligtenberg, S., Lenaerts, J., Van Den Broeke, M., and Scambos, T.: On the formation of blue ice on Byrd Glacier, Antarctica, Journal of Glaciology, 60, 41–50, https://doi.org/10.3189/2014JoG13J116, 2014.

Markov, A., Polyakov, S., Sun, B., Lukin, V., Popov, S., Yang, H., Zhang, T., Cui, X., Guo, J., Cui, P., et al.: The conditions of the formation and existence of “Blue Ice Areas” in the ice flow transition region from the Antarctic Ice Sheet to the Amery Ice Shelf in the Larsemann Hills area, Polar Science, 2019.

Marshall, G. J., Orr, A., van Lipzig, N. P. M., and King, J. C.: The Impact of a Changing Southern Hemisphere Annular Mode on Antarctic Peninsula Summer Temperatures, Journal of Climate, 19, 5388–5404, https://doi.org/10.1175/JCLI3844.1, https://doi.org/10.1175/JCLI3844.1, 2006.

Medley, B. and Thomas, E.: Increased snowfall over the Antarctic Ice Sheet mitigated twentieth-century sea-level rise, Nature Climate Change, 9, 34, 2019.

Medley, B., McConnell, J. R., Neumann, T., Reijmer, C., Chellman, N., Sigl, M., and Kipfstuhl, S.: Temperature and snowfall in western Queen Maud Land increasing faster than climate model projections, Geophysical Research Letters, 45, 1472–1480, 2018.

Morse, D. L., Waddington, E. D., and Steig, E. J.: Ice Age storm trajectories inferred from radar stratigraphy at Taylor Dome, Antarctica, Geophysical Research Letters, 25, 3383–3386, https://doi.org/10.1029/98GL52486, https://agupubs.onlinelibrary.wiley.com/doi/abs/10.1029/98GL52486, 1998.

Mouginot, J., Rignot, E., and Scheuchl, B.: Sustained increase in ice discharge from the Amundsen Sea Embayment, West Antarctica, from 1973 to 2013, Geophysical Research Letters, 41, 1576–1584, 2014.

Nicolas, J. P. and Bromwich, D. H.: New reconstruction of Antarctic near-surface temperatures: Multidecadal trends and reliability of global reanalyses, Journal of Climate, 27, 8070–8093, 2014.

Parish, T. R. and Bromwich, D. H.: The surface windfield over the Antarctic ice sheets, Nature, 328, 51, 1987.

https://doi.org/10.5194/tc-2020-36
Preprint. Discussion started: 11 February 2020

Parrenin, F., Petit, J.-R., Masson-Delmotte, V., Wolff, E., Basile-Doelsch, I., Jouzel, J., Lipenkov, V., Rasmussen, S., Schwander, J., Severi, M., et al.: Volcanic synchronisation between the EPICA Dome C and Vostok ice cores (Antarctica) 0–145 kyr BP, Climate of the Past, 8, 1031–1045, https://doi.org/10.5194/cp-8-1031-2012, 2012.

Pörtner, H.-O., Roberts, D., Masson-Delmotte, V., Zhai, P., Tignor, M., Poloczanska, E., Mintenbeck, K., Nicolai, M., Okem, A., Petzold, J., Rama, B., and Weyer, N.: IPCC, 2019: Summary for Policymakers., Cambridge University Press, in press.

Rayner, N., Parker, D. E., Horton, E., Folland, C. K., Alexander, L. V., Rowell, D., Kent, E., and Kaplan, A.: Global analyses of sea surface temperature, sea ice, and night marine air temperature since the late nineteenth century, Journal of Geophysical Research: Atmospheres, 108, 2003.

Rignot, E., Mouginot, J., Scheuchl, B., van den Broeke, M., van Wessem, M. J., and Morlighem, M.: Four decades of Antarctic Ice Sheet mass balance from 1979–2017, Proceedings of the National Academy of Sciences, 116, 1095–1103, 2019.

Scambos, T., Frezzotti, M., Haran, T., Bohlander, J., Lenaerts, J., Van Den Broeke, M., Jezek, K., Long, D., Urbini, S., Farness, K., and et al.: Extent of low-accumulation 'wind glaze' areas on the East Antarctic plateau: implications for continental ice mass balance, Journal of Glaciology, 58, 633–647, https://doi.org/10.3189/2012JoG11J232, 2012.

Scarchilli, C., Frezzotti, M., and Ruti, P. M.: Snow precipitation at four ice core sites in East Antarctica: provenance, seasonality and blocking factors, Climate dynamics, 37, 2107–2125, 2011.

Shepherd, A., Ivins, E., Rignot, E., Smith, B., Van Den Broeke, M., Velicogna, I., Whitehouse, P., Briggs, K., Joughin, I., Krinner, G., et al.: Mass balance of the Antarctic Ice Sheet from 1992 to 2017, Nature, 558, 219–222, 2018.

Sjolte, J., Sturm, C., Adolphi, F., Vinther, B. M., Werner, M., Lohmann, G., and Muscheler, R.: Solar and volcanic forcing of North Atlantic climate inferred from a process-based reconstruction, Climate of the Past, 14, 1179–1194, https://doi.org/10.5194/cp-14-1179-2018, https://www.clim-past.net/14/1179/2018/, 2018.

Sodemann, H. and Stohl, A.: Asymmetries in the moisture origin of Antarctic precipitation, Geophysical Research Letters, 36, https://doi.org/10.1029/2009GL040242, https://agupubs.onlinelibrary.wiley.com/doi/abs/10.1029/2009GL040242, 2009.

Spaulding, N. E., Spikes, V. B., Hamilton, G. S., Mayewski, P. A., Dunbar, N. W., Harvey, R. P., Schutt, J., and Kurbatov, A. V.: Ice motion and mass balance at the Allan Hills blue-ice area, Antarctica, with implications for paleoclimate reconstructions, Journal of Glaciology, 58, 399–406, 2012.

Steiger, N. J., Steig, E. J., Dee, S. G., Roe, G. H., and Hakim, G. J.: Climate reconstruction using data assimilation of water isotope ratios from ice cores, Journal of Geophysical Research: Atmospheres, 122, 1545–1568, 2017.

Stenni, B., Serra, F., Frezzotti, M., Maggi, V., Traversi, R., Becagli, S., and Udisti, R.: Snow accumulation rates in northern Victoria Land, Antarctica, by firn-core analysis, Journal of Glaciology, 46, 541–552, 2000.

Stenni, B., Curran, M. A. J., Abram, N. J., Orsi, A., Goursaud, S., Masson-Delmotte, V., Neukom, R., Goosse, H., Divine, D., van Ommen, T., Steig, E. J., Dixon, D. A., Thomas, E. R., Bertler, N. A. N., Isaksson, E., Ekaykin, A., Werner, M., and Frezzotti, M.: Antarctic climate variability on regional and continental scales over the last 2000 years, Climate of the Past, 13, 1609–1634, https://doi.org/10.5194/cp-13-1609-2017, https://www.clim-past.net/13/1609/2017/, 2017.

Stocker, T. F., Qin, D., Plattner, G.-K., Tignor, M., Allen, S. K., Boschung, J., Nauels, A., Xia, Y., Bex, V., and Midgley, P. M.: Climate change 2013: The physical science basis, Cambridge Univ Press, New York, 2013.

Thomas, E. R., Marshall, G. J., and McConnell, J. R.: A doubling in snow accumulation in the western Antarctic Peninsula since 1850, Geophysical research letters, 35, 2008.

https://doi.org/10.5194/tc-2020-36
Preprint. Discussion started: 11 February 2020

590 Thomas, E. R., Hosking, J. S., Tuckwell, R. R., Warren, R., and Ludlow, E.: Twentieth century increase in snowfall in coastal West Antarctica, Geophysical Research Letters, 42, 9387–9393, 2015.

Thomas, E. R., van Wessem, J. M., Roberts, J., Isaksson, E., Schlosser, E., Fudge, T. J., Vallelonga, P., Medley, B., Lenaerts, J., Bertler, N., van den Broeke, M. R., Dixon, D. A., Frezzotti, M., Stenni, B., Curran, M., and Ekaykin, A. A.: Regional Antarctic snow accumulation over the past 1000 years, Climate of the Past, 13, 1491–1513, https://doi.org/10.5194/cp-13-1491-2017, https://www.clim-past.net/13/
595 1491/2017/, 2017.

Turner, J., Lu, H., White, I., King, J. C., Phillips, T., Hosking, J. S., Bracegirdle, T. J., Marshall, G. J., Mulvaney, R., and Deb, P.: Absence of 21st century warming on Antarctic Peninsula consistent with natural variability, Nature, 535, 411, 2016.

Turner, J., Phillips, T., Thamban, M., Rahaman, W., Marshall, G. J., Wille, J. D., Favier, V., Winton, V. H. L., Thomas, E., Wang, Z., et al.: The Dominant Role of Extreme Precipitation Events in Antarctic Snowfall Variability, Geophysical Research Letters, 46, 3502–3511,
600 2019.

Turton, J. V., Kirchgaessner, A., Ross, A. N., and King, J. C.: Does high-resolution modelling improve the spatial analysis of föhn flow over the Larsen C Ice Shelf?, Weather, 72, 192–196, https://doi.org/10.1002/wea.3028, https://rmets.onlinelibrary.wiley.com/doi/abs/10.1002/wea.3028, 2017.

Unden, P., Rontu, L., Järvinen, H., Lynch, P., Calvo, J., Cats, G., Cuxart, J., Eerola, K., Fortelius, C., Garcia-Moya, J. A., Jones, C., Geert,
605 Lenderlink, G., Mcdonald, A., Mcgrath, R., Navascues, B., Nielsen, N. W., Degaard, V., Rodriguez, E., Rummukainen, M., Sattler, K., Sass, B. H., Savijarvi, H., Schreur, B. W., Sigg, R., and The, H.: HIRLAM-5 Scientific Documentation, 2002.

Urbini, S., Frezzotti, M., Gandolfi, S., Vincent, C., Scarchilli, C., Vittuari, L., and Fily, M.: Historical behaviour of Dome C and Talos Dome (East Antarctica) as investigated by snow accumulation and ice velocity measurements, global and planetary change, 60, 576–588, 2008.

van den Broeke, M. R., van Lipzig, N. P. M., and van Meijgaard, E.: Momentum Budget of the East Antarctic Atmospheric Bound-
610 ary Layer: Results of a Regional Climate Model, Journal of the Atmospheric Sciences, 59, 3117–3129, https://doi.org/10.1175/1520-0469(2002)059<3117:MBOTEA>2.0.CO;2, https://doi.org/10.1175/1520-0469(2002)059<3117:MBOTEA>2.0.CO;2, 2002.

Van Wessem, J. M., Jan Van De Berg, W., Noël, B. P., Van Meijgaard, E., Amory, C., Birnbaum, G., Jakobs, C. L., Krüger, K., Lenaerts, J., Lhermitte, S., et al.: Modelling the climate and surface mass balance of polar ice sheets using RACMO2: Part 2: Antarctica (1979-2016), The Cryosphere, 12, 1479–1498, 2018.

615 Wang, H., Fyke, J., Lenaerts, J., Nusbaumer, J., Singh, H., Noone, D., and Rasch, P.: Influence of Sea Ice Anomalies on Antarctic Precipitation Using Source Attribution, The Cryosphere Discussions, 2019, 1–27, https://doi.org/10.5194/tc-2019-69, https://www.the-cryosphere-discuss.net/tc-2019-69/, 2019.

Wang, Y., Ding, M., van Wessem, J. M., Schlosser, E., Altnau, S., van den Broeke, M. R., Lenaerts, J. T. M., Thomas, E. R., Isaksson, E., Wang, J., and Sun, W.: A Comparison of Antarctic Ice Sheet Surface Mass Balance from Atmospheric Climate Models and In Situ
620 Observations, Journal of Climate, 29, 5317–5337, https://doi.org/10.1175/JCLI-D-15-0642.1, https://doi.org/10.1175/JCLI-D-15-0642.1, 2016.

Whillans, I. M.: Effect of inversion winds on topographic detail and mass balance on inland ice sheets, Journal of Glaciology, 14, 85–90, 1975.